Structure of the Molten 37 a/o Cu-63 a/o Sb Alloy Using the Isotopic Substitution Method in Neutron Diffraction

W. Knoll* and S. Steeb

Max-Planck-Institut für Metallforschung, Institut für Werkstoffwissenschaften, Stuttgart

Z. Naturforsch. **33a**, 472–479 (1978); received February 26, 1978

A neutron diffraction study of the eutectic Cu-Sb-melt containing 37 a/o Cu has been performed using isotopically enriched samples. The three partial structure factors describing the Cu-Cu, Cu-Sb, and Sb-Sb correlations have been determined as well as a second set of partial structure factors relating to the distance correlation of fluctuations in number density and concentration.

Unsmoothed total structure factors were used. By Fourier-transformation the corresponding pair correlation functions were obtained. A strong segregation tendency was found. Concentration fluctuations with a correlation length of 2.4 Å could be determined. From the Fourier-transform of S_{CC} the product $\overline{N}_1\alpha_1$ was obtained confirming the segregation tendency. The distance of nearest Cu-Cu neighbours in the eutectic Cu-Sb melt was found to be smaller than in pure molten Cu, whereas the Sb-Sb distance is larger than in pure Sb.

According to Faber-Ziman theory the electrical resistivity was calculated and compared with experimental data.

1. Introduction

The object of this paper is to report on an experimental study of the structure of a molten Cu-Sb-alloy containing 37 a/o Cu using the isotopic substitution method in a neutron diffraction experiment. Recent progresses in the experimental technique and the availability of Cu-isotopes encouraged a new determination of the partial structure factors of the eutectic composition, where segregation tendency in the melt had been stated in a former work [1, 2].

2. Theoretical Outline

From a single neutron diffraction experiment the total structure factor $S(Q)$ can be obtained. For a binary alloy this structure factor is the weighted sum of three partial structure factors:

$$\begin{aligned}\langle b^2\rangle (S(Q)-1) = {} & c_1^2 b_1^2 (S_{11}(Q)-1) \\ & + c_2^2 b_2^2 (S_{22}(Q)-1) \\ & + 2 c_1 c_2 b_1 b_2 (S_{12}(Q)-1)\end{aligned} \quad (1)$$

with

b_1, b_2 = neutron scattering lengths of the two species 1, 2,

c_1, c_2 = atomic concentrations ($c_1 + c_2 = 1$),

S_{ij} = partial structure factors, according to Ref. [3],

i, j = 1 or 2.

The partial structure factors are related to the radial distribution functions g_{ij} by

$$Q(S_{ij}(Q)-1) = 4\pi\varrho_0 \int_0^\infty (g_{ij}(r)-1)\, r \sin Qr \, \mathrm{d}r \quad (2)$$

with ϱ_0 = mean number density.

Another set of partial structure factors, S_{NN}, S_{CC}, S_{NC} has been introduced by Bhatia and Thornton [4] according to which the total structure factor can be written as

$$\begin{aligned}\langle b^2\rangle S(Q) = {} & \langle b\rangle^2 S_{NN}(Q) + \Delta b^2 S_{CC}(Q) \\ & + 2\langle b\rangle \Delta b\, S_{NC}(Q)\end{aligned} \quad (3)$$

with $\langle b^2\rangle = c_1 b_1^2 + c_2 b_2^2$,
$\langle b\rangle = c_1 b_1 + c_2 b_2$,
$\Delta b = b_1 - b_2$.

For liquid alloys these structure factors in the long wavelength limit ($Q \to 0$) are related to thermodynamic quantities:

$$S_{CC}(0) = N k_B T \Big/ \frac{\partial^2 G}{\partial c^2} = \frac{c_j a_i}{\partial a_i / \partial c_i}, \quad (4)$$

$$S_{NN}(0) = \varrho_0 k_B T \beta_{is} + \delta^2 S_{CC}(0), \quad (5)$$

$$S_{NC}(0) = -\delta S_{CC}(0) \quad (6)$$

Reprint requests to Prof. Dr. S. Steeb, MPI für Metallforschung, Institut für Werkstoffwissenschaften, Seestraße 92, D-7000 Stuttgart 1.

* Work performed at the Institute Laue-Langevin, Grenoble, France.

where β_{is} = isothermal compressibility,
$\delta = \varrho_0(v_1 - v_2)$,
a_i = thermodynamic activity,
v_i = partial molar volume.

From Eqs. (3)—(6) follows

$$\langle b^2\rangle S(0) = \langle b\rangle^2 \varrho_0 k_B T \beta_{is} + (\langle b\rangle \delta - \Delta b)^2 S_{CC}(0) . \quad (7)$$

$S_{CC}(0)$ may thus be calculated according to Eq. (4) from thermodynamic data or according to Eq. (7) from the diffraction experiment. The partial structure factors, either S_{11}, S_{22}, S_{12} or S_{NN}, S_{CC}, S_{NC}, can be obtained by varying the scattering lengths of one or both components in such a way as to provide three total structure factors S_I, S_{II}, and S_{III}, which are sufficiently different to enable three linear equations to be solved for the S_{ij} ($i, j = 1$ or 2, N or C). The problems occuring with the resolution of a system of three equations as Eq. (1) or (3) are fully discussed in [5] and will be considered in the experimental part of this work as well.

3. Experimental

The samples were prepared from 6 N Antimony*, from 5 N natural Copper*, and from the following isotopes**: 97.4% enriched Copper 63 and 93.9% enriched Copper 65 (according to mass spectrometric analysis of the manufacturer). The alloys with 37 a/o Cu and 63 a/o Sb were sealed under vacuum into quartz tubes with an inner diameter of 8.6 mm and a wall thickness of 0.5 mm. The measurements were carried out at the D 4-instrument of the Institute Laue-Langevin, Grenoble, France. The cross section of the neutron beam of 0.696 Å wavelength was 47×13 mm^2 for the 37 Cu^{nat}-63 Sb and for the 37 Cu^{63}-63 Sb sample, whereas for the 37 Cu^{65}-63 Sb due to the smaller quantity of Cu^{65} a beam of 29×13 mm^2 was chosen. The irradiated volume of the samples was defined to better than 0.3% by boron nitride screens. The samples were held in a vertical cylindrical V-foil resistivity furnace. The temperature of 873 K was measured with a Chromel-Alumel thermocouple and stabilized to better than ± 1 degree by a PID-thyristor controller.

* Fa. Fluka AG, Buchs/Switzerland.
** Rohstoff Einfuhr GmbH, Düsseldorf/Germany.

The scattered neutrons were detected by a single He^3-counter at 140 cm from the center of the goniometer, the receiving slit being 50×20 mm^2. Intensities were measured in an angular range corresponding to $0.19 \leqq Q \leqq 15$ Å^{-1} for the sample, the empty container, the furnace, and the background. For calibration and small angle correction further runs were made using a Vanadium rod and a Cd-rod with the same dimensions as the sample. Different monitor presets were used to obtain the same total number of counts at great Q-values for all three samples, taking into account the different total scattering cross sections (see Table 1). The statistical error for each sample was less than 0.5%. In the range of 0.19 Å$^{-1} \leqq Q \leqq 7$ Å^{-1}, a step-width of 0.2° in 2θ was chosen, for greater Q-values steps of 0.9° were used. The measurements at the latter momentum transfers were taken for calibration and consistency checks only.

4. Corrections

In order to obtain the effective scattering from the sample, in a first step, corrections for background with closed beam, container, furnace, and absorption were performed. The corrected scattering intensity from the sample alone I^{corr} is given by

$$I^{corr} = A_1[I_S - A_2 I_C - A_3 I_F] \quad (9)$$

with

I_S = Intensity obtained from the sample in the container and in the furnace,

I_C = Intensity obtained from the container in the furnace,

I_F = Intensity obtained from the empty furnace.

All these intensities are net intensities, i.e. with background intensity subtracted. The absorption correction factors A_1, A_2, and A_3 were calculated by the equations and the program given by Poncet [6], which takes properly into account the contribution of the furnace not being fully bathed in the neutron beam. The absorption factors A_1 and A_2 tend for a disappearing cross section and thickness of the furnace material towards the well known Paalman and Pings [7] factors.

A further correction is necessary in the small angle region, where air scattering and scattering from slits along the primary beam as well as divergency of the primary beam occurs. The corresponding contribution to the intensity has to

be measured and subtracted. Therefore the specimen plus container is replaced by a Cd-rod, so that only neutrons which wouldn't interact with the sample and the container reach the counter. The small angle intensity I_{Cd} thus obtained reaches a minimum I_{min} at about $Q = 1.5$ Å^{-1} and becomes larger for larger Q-values, since scattering from the illuminated part of the Cd-rod occurs. The intensity to be subtracted in the small angle region is obtained according to $I'_{Cd} = I_{Cd} - I_{min}$. For each run (sample, container, furnace) this quantity I'_{Cd} has to be subtracted and Eq. (9) becomes for 0.19 Å^{-1} $\leqq Q \leqq 1.5$ Å^{-1}

$$I^{corr} = A_1[I_S - A_2 I_C - A_3 I_F - (1 - A_2 - A_3) I'_{Cd}]. \quad (9')$$

For Q-values greater than 1.5 Å^{-1}, I'_{Cd} is set to zero and Eq. (9') and (9) become identical. It should be mentioned, that this method applied for the V-rod measurement after a further consideration of inelasticity, yields an absolutely angle independent corrected intensity.

The corrected intensity I^{corr} now is the total scattering from the sample. In order to obtain the coherent scattering, a correction for multiple scattering was applied using the isotropic approximation of Blech and Averbach [8]. A correction for inelasticity effects was performed as calculated in [9] and already described for a D4-experiment by Bertagnolli et al. [10].

Finally a calibration by the Vanadium run, corrected in the same way was done in order to obtain the coherent scattered intensities in an absolute scale.

5. Coherent Scattering Lengths and Consistency Checks

For the coherent scattering length of Cu^{nat} two values are given in literature, namely $0.76 \cdot 10^{-12}$ cm/atom or $0.79 \cdot 10^{-12}$ cm/atom (see Ref. [11, 12]). For each of the two stable isotopes, namely Cu^{63} and Cu^{65}, to our knowledge the unique given values are 0.67 and 1.11×10^{-12} cm/atom. The recalculation of b_{coh}^{nat} from the scattering lengths of the two isotopes leads to a value of $0.806 \cdot 10^{-12}$ cm/atom. Thus a discrepancy of two to six percent to the tabulated values must be stated. Regarding the natural abundance of the two isotopes, for the following the assumption will be made, that the discrepancy may be due to an error in the tabulated value of the scattering length of Cu^{65}.

Assuming the value of $0.79 \cdot 10^{-12}$ cm/atom as valid for Cu^{nat}, recalculation yields $1.06 \cdot 10^{-12}$ cm/atom for Cu^{65}, a value 5% less than the tabulated one. The scattering data of the natural elements and isotopes used in the present work are given in Table 1.

For the three samples with the data from Table 1 the coherent scattering cross section $\sigma_{coh} = 4\pi\langle b\rangle^2$, the total scattering cross section $\sigma_{sc} = 4\pi\langle b^2\rangle$, the incoherent scatttering cross section $\sigma_{inc} = \sum c_i \sigma_{inc}^i$ with $i =$ Cu or Sb, respectively, the absorption cross section $\sigma_{abs} = c_i \sigma_{abs}^i$, the total cross section $\sigma_{total} = \sigma_{sc} + \sigma_{inc} + \sigma_{abs}$, and the macroscopic attenuation coefficient $\mu = \sigma_{total} \cdot \varrho_0$ with $\varrho_0 =$ mean number density were calculated and are given in Table 2. This table contains also the multiple scattering cross section σ_{mult} calculated according to [8] and the long wavelength limit total structure factor $S_{calc}(0)$ calculated from thermodynamical data [14].

For a consistency check, from the total scattered intensities (sc + inc + mult) at great Q-values for all three samples the corresponding scattering cross sections with the Vanadium standard were calculated. The difference in the sum of $\sigma_{sc} + \sigma_{inc} + \sigma_{mult}$ between the values listed in Table 2 and the values calculated from the experiment never exceeded 0.6%. This is a very good agreement, the small difference may already be explained by errors in the sample volume for example.

	b_{coh} [10^{-12} cm · atom^{-1}]	σ_{inc} [barn]	σ_{abs} [barn] ($\lambda = 0{,}696$ Å)
Cu^{nat}	0.79	0.4	1.5
Cu^{63}	0.67	0	1.8
Cu^{65}	1.06	0	0.87
0.974 Cu^{63} 0.026 Cu^{65}	0.68	0.05	1.7
0.939 Cu^{65} 0.061 Cu^{63}	1.036	0.11	0.9
Sb (Ref. [13])	0.54	0.2	2.1

Table 1. Scattering data for the elements and the used isotopes.

It has to be stated here, however, that this agreement could be obtained only by making the assumption that the coherent scattering length of the Cu 65-isotope given in the literature is too large. Using the "literature-value" of $b_{Cu}^{65} = 1.11 \cdot 10^{-12}$ cm a difference of $\approx 5\%$ would occur between the tabulated and the experimentally determined sum of $\sigma_{sc} + \sigma_{inc} + \sigma_{melt}$. This error certainly exceeds the possible errors under the actual experimental conditions, therefore the adjusted value for $b_{Cu}^{65} = 1.06 \cdot 10^{-12}$ cm was found to be matching the experiment in a most reliable way, and it might be interesting to perform a new determination of the scattering length of both, the copper isotopes and the natural Cu.

6. Results and Discussion

Total Structure Factors

From the three samples listed in Table 2 according to Chapter 4 the corrected coherent scattered intensities in absolute units were obtained and from these the total structure factors $S(Q)$ were calculated according to [1].

In Figure 1 the total structure factors for the three alloys are given in the range $0.19 \leqq Q \leqq 7$ Å^{-1}. No smoothing of the measured values has been performed, thus the given points contain the statistical error. The curves are arranged in such a way, that from top to bottom the Cu scattering length decreases. Marked differences occur in the shape of the first peak. The shoulder on the left side of the first maximum of the structure factor from the Cu^{65}-Sb-alloy obtains more weight for the case of the Cu^{nat}-Sb and the Cu^{63}-Sb-alloy. This indicates clearly, that with decreasing scattering cross section of Copper, the antimony-contribution to the total structure factor increases. This shoulder on the left part of the first peak is situated at about 2.25 Å^{-1}. In pure Sb, the first peak lies at 2.2 Å^{-1} [1].

The right part of the first maximum lies at 2.98 Å^{-1} for all three structure factors in Fig. 1, in [1] for liquid Cu a value of 3.02 Å^{-1} was obtained.

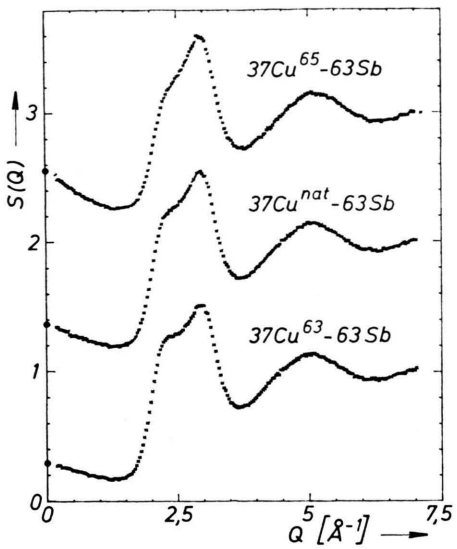

Fig. 1. Molten 37 a/o Cu-63 a/o Sb: Total Structure Factors.

The Q-values for the two parts of the first peak found here agree perfectly with the structure factor of the same alloy measured in [1]. A great difference, however, occurs for small Q-values, where the three structure factors show a rise towards $Q \to 0$. This had not been detected in the earlier work [1] due to the limited range of detection of the instrument used. On the ordinate of Fig. 1 three full circles indicate the long-wavelength-limits of the total interference function $S(Q)$ tabulated in Table 2. The extrapolation of the measured $S(Q)$ in Fig. 1 shows an excellent agreement. The rise in the structure factors for $Q \to 0$ is explained by concentration fluctuations. An Ornstein-Zernike [15] plot of the inverse absolute intensities for the Cu^{65}-Sb- and Cu^{nat}-Sb-alloy versus Q^2 yields a correlation length of about 2.4 Å and confirms the segregation tendency in the 37 Cu-63 Sb melt already stated in [1].

Partial Structure Factors

By direct solution of the system of three linear equations (1), the three partial structure factors

Table 2. Quantities used during data evaluation.

Sample	σ_{coh} [barn]	σ_{sc} [barn]	σ_{inc} [barn]	σ_{abs} [barn]	σ_{total} [barn]	μ [cm^{-1}]	σ_{mult} [barn]	$S_{calc}(0)$
0.37 Cu^{nat} 0.63 Sb	5.03	5.21	0.28	1.85	7.34	0.313	0.62	0.46 ± 0.12
0.37 Cu^{63} 0.63 Sb	4.4	4.46	0.14	1.93	6.53	0.280	0.44	0.35 ± 0.09
0.37 Cu^{65} 0.63 Sb	6.58	7.30	0.17	1.64	9.11	0.378	1.07	0.59 ± 0.15

S_{Sb-Sb}, S_{Cu-Sb} and S_{Cu-Cu} were calculated. They are shown in Fig. 2 as the zig-zag lines. The "band widths" of these curves indicate the error due to the statistical or systematic errors in the total structure factors.

Though the value of the normalized determinant [16] of the system of three linear equations (1) or (3) has the very small value of $|D| = 0.003$, the direct solution yields quite good resulting partial structure factors. The uncertainty for each point is $S_{ij}(Q) \pm 1.1$.

The solid lines in Fig. 2 represent a cubic splinefit for the partial structure factors. It may be pointed out here, that the determination of the partial structure factors was possible only by using the unsmoothed total $S(Q)$. In other works, like in the case of CuCl, Page and Mika [17] used a cubic splinefit for the total $S(Q)$, in the case of KCl and CsCl, Derrien and Dupuy [18] used handfitted total $S(Q)$.

Using splinefitted total $S(Q)$ in the present work, the partial structure factors shown in Fig. 3 were obtained. A lot of ripples shows clearly the drastic influence of very small errors in the fits. No smooth curve with a physical meaning can be drawn through these partials, they even do not fullfill the sum rule especially in the case of S_{Sb-Sb}. It may be interesting here, to note that in [18] similar unphysical ripple-structure of the partials was

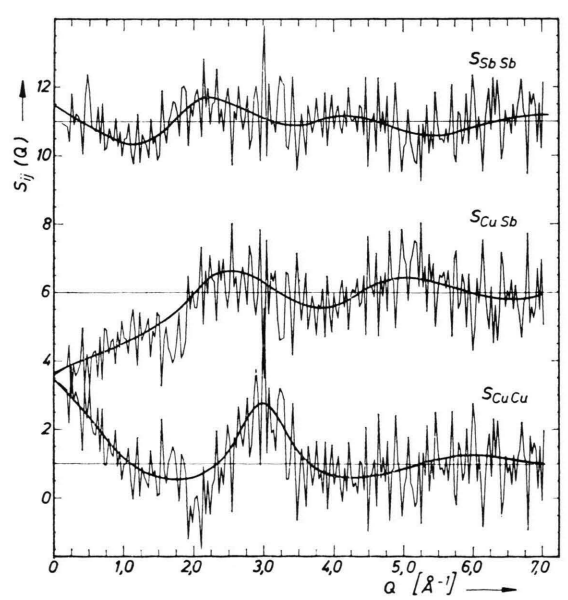

Fig. 2. Partial structure factors S_{Cu-Cu}, S_{Cu-Sb}, and S_{Sb-Sb}.

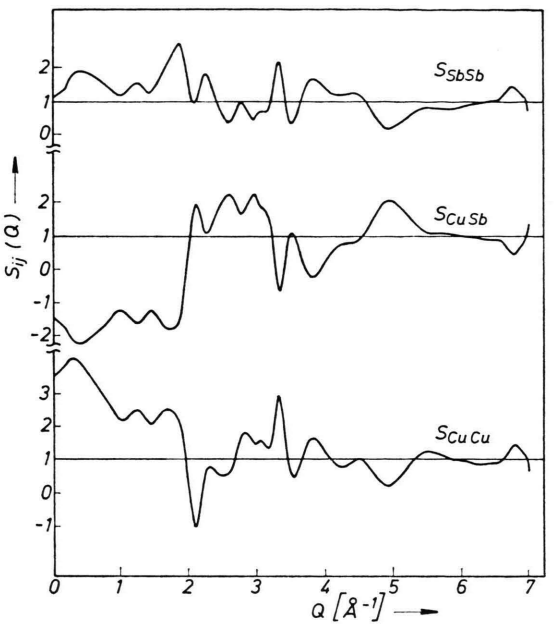

Fig. 3. Incorrect set of partial structure factors S_{Cu-Cu}, S_{Cu-Sb}, and S_{Sb-Sb} obtained from smoothed total $S(Q)$.

obtained. A Fourier-transformation of splinefitted total $S(Q)$ however, yields absolutely the same pair correlation function $g(r)$ as a Fourier-transformation of unsmoothed total $S(Q)$. The partial $S_{ij}(Q)$ in Fig. 2 fullfill the sum rule condition which was found to be very sensitive on errors in the total $S(Q)$. A y-shift of one $S(Q)$ of only 0.3% for example, yields a value for the atomic density obtained from the sum rule integral, which is at least wrong by a factor of 10. In the further discussion only the partial $S_{ij}(Q)$ of Fig. 2 will be used.

The partial function S_{Cu-Cu} in Fig. 2 shows a first peak at 3 Å^{-1}, this is the same value within the errors, as for pure molten Cu. The same coincidence can be stated for S_{Sb-Sb} and pure Sb. The second peak in the $S(Q)$ of Sb at 3.1 Å^{-1} reported in [1], however, is not present. A comparison of the structure factors determined here and those reported in an earlier work [2] shows a similar result concerning S_{Cu-Cu} except the small Q-part, where a steep rise is found now, due to concentration fluctuations.

The functions S_{Cu-Sb} are not very similar, the first peak of the "new" structure factor occurs at 2.6 Å^{-1}, whereas in [2] 2.95 Å^{-1} were given.

For S_{Sb-Sb} in this work a first peak is at 2.3 Å^{-1} as found in [2], a second peak, however, immediately

following the first maximum at 4.25 $Å^{-1}$ was not reported in [2]. As a conclusion it may be stated, that the structure factors, determined by the isotopic substitution method differ quite clearly from those derived under the assumption of concentration independency in [2]. Using the pseudopotentials for Cu and Sb given by Animalu [19] for a calculation of the electrical resistivity according to the Faber-Ziman formula, a value of 99.5 μΩ cm was obtained. The measured value [20] for the resistivity is 102 μΩ cm.

By direct solution of the system of three linear equations (3) the Bhatia-Thornton structure factors for the 37 Cu-63 Sb alloy were determined and are shown in Figure 4. The solid lines represent, as in Figure 2, the best fit curves, using a cubic spline for the partial functions. The partial $S_{NN}(Q)$ is the Fourier-transform of the distance correlation of local Cu and Sb atom number density fluctuations. As to be expected, this curve shows a strong resemblance with the total structure factors in Fig. 1, the positions of the double headed first peak are situated at about the same values of 2.25 and 3 $Å^{-1}$. The rise of S_{NN} towards small Q values is almost negligible, it can be seen, that the rise of the total structure factors at small Q-values is due to concentration fluctuations only. The corresponding quantity, S_{CC}, is the Fourier-transform of the distance correlation of concentration fluctuations. Though S_{CC} shows a great statistical error, a rise towards small Q-values proves the existence of concentration fluctuations in the melt. The correlation length of these fluctuations has already been determined from the total $S(Q)$. S_{CC} oscillates properly around the value $c_{Cu}c_{Sb}$ as required from theory, the oscillations, however, are very weak.

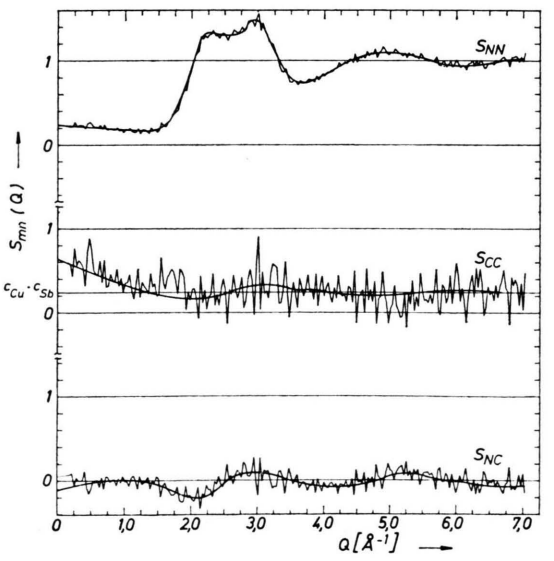

Fig. 4. Partial structure factors S_{NN}, S_{CC}, and S_{NC}.

The partial $S_{NC}(Q)$ oscillates around zero. It is the Fourier-transform of the cross correlation between density and concentration fluctuations. It should vanish for an alloy with atoms of equal size, where the arrangement of 1 and 2 atoms around a 1 atom is the same as around a 2 atom. This condition has first been introduced by Keating [21]. In the case of 37 Cu-63 Sb S_{NC} does not vanish, thus indicating a size effect. This is a quite evident result for the two species Cu and Sb.

Pair Correlation Functions

By Fourier-transformation of the total $S(Q)$, the total pair correlation functions $g(r)$ of Fig. 5 were obtained. For all three samples in a first view

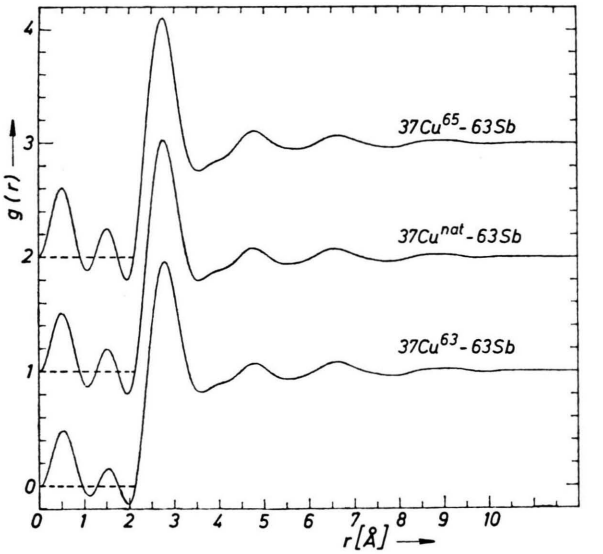

Fig. 5. Molten 37 a/o Cu-63 a/o Sb: Total pair correlation functions.

almost the same $g(r)$ was found. There are, however, small differences in the position of the first peak r_I varying from 2.73 Å to 2.77 Å and 2.79 Å for the samples with decreasing Cu-scattering length, due to the different weight of the pair distances occurring in the different melts. These differences are quite small and are just beyond the estimated error

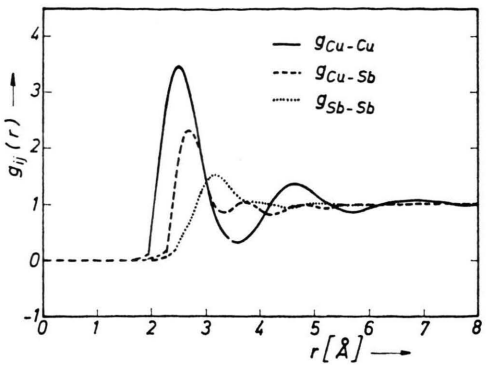

Fig. 6. Partial pair correlation functions.

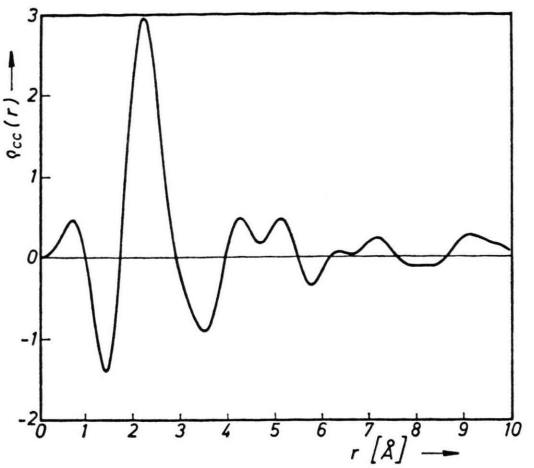

Fig. 7. Concentration correlation function.

of ± 0.02 Å in the determination of the position of the first peak. The number of first neighbours was found to be $N_I = 6.8 \pm 0.2$ atoms for all three samples. A comparison with the same alloy containing natural Copper investigated earlier [1] shows an excellent agreement, $r_I = 2.76$ Å and $N_I = 7$ atoms have been reported there. The partial structure factors of Fig. 2 have been Fourier-transformed as well, the resulting $g(r)$ are shown in Figure 6. The position of $r_I = 2.55$ Å in g_{Cu-Cu} is smaller than the corresponding value of 2.61 Å obtained in [1] for pure Cu, whereas for g_{Sb-Sb} a value of 3.2 Å, which is greater than that of molten Sb, with 3.08 Å, was found. As to be expected, the first peak position of g_{Cu-Sb} gives an intermediate value of 2.7 Å.

In comparison with the partial pair correlation functions reported in [2] it can be stated, that the new g_{Cu-Sb} and g_{Sb-Sb} are much more damped than those determined with the assumption of concentration independence. Beyond the first peak no more significant oscillations in both $g(r)$-curves can be detected, if the possible uncertainty is taken into account. Thus, besides the first neighbours no preferred distance occurs, and an absolutely statistical distribution of Sb-Sb and Cu-Sb pairs in the melt may be supposed for all distances larger than r_I. The function g_{Cu-Cu}, however, shows still a pronounced second and third neighbour-shell and is quite similar to the g_{Cu-Cu} reported in [2] and to the $g(r)$ of pure liquid Copper [1]. A recalculation according to Ref. [2] of the total $g(r)$ by the weighted sum of the partial functions of Fig. 6 yields quite good agreement up to 8 Å.

By Fourier-transformation of $S_{CC}(Q)$ (Fig. 4), the so called radial concentration-correlation function $\varrho_{CC}(r)$ was obtained. This function, which is shown in Fig. 7, has first been introduced in [22] and is fully discussed in [23]. The integral over the first peak yields:

$$\int_{r_1-\varepsilon}^{r_1+\varepsilon} 4\pi r^2 \varrho_{CC}(r)\,dr = \bar{N}_1 \alpha_1 \tag{10}$$

with $\bar{N}_1$ = real number of atoms in the first coordination sphere, and α_1, the short range order coefficient. $\bar{N}_1\alpha_1$ is found to be 4.3 ± 0.3. The positive value of the short range order parameter gives an additional proof for the segregation tendency in the melt under investigation.

[1] W. Knoll and S. Steeb, Phys. Chem. Liquids **4**, 39 (1973).
[2] W. Knoll and S. Steeb, Phys. Chem. Liquids **4**, 27 (1973).
[3] T. E. Faber and J. M. Ziman, Phil. Mag. **11**, 153 (1965).
[4] A. B. Bhatia and D. E. Thornton, Phys. Rev. **B2**, 3004 (1970).
[5] F. G. Edwards, J. E. Enderby, R. A. Howe, and D. I. Page, J. Phys. **C8**, 3483 (1975).
[6] P. F. J. Poncet, Thesis work, University of Reading, UK, 1976.
[7] H. H. Paalman, C. J. Pings, J. Appl. Phys. **33**, 2635 (1962).
[8] I. A. Blech and B. L. Averbach, Phys. Rev. **137**, A 1113 (1965).
[9] J. L. Yarnell et al, Phys. Rev. **7**, A 2130 (1973).
[10] H. Bertagnolli, P. Chieux, and M. D. Zeidler, Mol. Phys. **32**, 759 (1976).
[11] D. T. Keating et al, Phys. Rev. **111**, 261 (1958).
[12] G. F. Bacon, Neutron Diffraction 3rd edition, Clarendon Press, Oxford (1975),
[13] G. Arnold, N. Nereson, Phys. Rev. **131**, 2098 (1963).

[14] R. Hultgren et al, Selected values of the thermodynamic properties of binary alloys (1973), American Society for Metals, Ohio, USA.
[15] L. S. Ornstein and F. Zernike, Phys. Z. **19**, 134 (1918).
[16] J. R. Westlake, A Handbook of Numerical Matrix Inversion, John Wiley, New York 1968.
[17] D. I. Page and K. Mika, J. Phys. Chem. **4**, 3034 (1971).
[18] J. Y. Derrien and J. Dupuy, J. Phys. Paris **36**, 191 (1975).
[19] A. O. E. Animalu, Solid State Theory Group, Cavendish Lab., UK, Technical report no. 3 (1965) and private communication.
[20] S. Steeb, U. Maier, and D. Godel, Phys. Chem. Liquids **1**, 221 (1969).
[21] D. T. Keating, J. Appl. Phys. **34**, 923 (1963).
[22] H. Ruppersberg and H. Egger, J. Chem. Phys. **63**, 4095 (1975).
[23] A. Boos, P. Lamparter, and S. Steeb, Z. Naturforsch. **32A**, 1222 (1977).